Oscillatory relativistic motion of a particle in a power-law or sinusoidal-shaped potential well

Denis Teychenné and Guy Bonnaud
Commissariat á l'Energie Atomique, Centre d'Etudes de Limeil-Valenton, 94195 Villeneuve-Saint-Georges, France

Jean-Louis Bobin
Université Pierre & Marie Curie, Tour 13, E5, 75252 Paris, France
(Received 23 July 1993)

We report on an analytical work about the one-dimensional undamped relativistic motion of a particle located in a potential well whose space dependence is given by a power law or a sinusoidal law. This analysis is of interest in the present-day research field on interaction of ultra-high-intensity laser pulses with plasmas. First, we consider the oscillating motion of a particle trapped inside a potential-energy profile of the form $K|x|^n$ where K is a constant, x is the space coordinate, and n is a positive real number. The cases $n=1$ and $n=2$ are emphasized since the former is related to the motion of electrons that exit an homogeneous electrically neutral plasma towards vacuum and the latter is related to the usual electron plasma oscillation. Second, we study the potential-energy profile $\cos(x)$ in connection with the acceleration of an electron inside an electron plasma wave. Both trapped and untrapped particle motions are considered. For all the potential-energy shapes, analytic expressions of both the period of the oscillating motion and the particle trajectory are provided. The particle motion in the weakly relativistic case is discussed. The acceleration length of a particle trapped inside a sinusoidal drifting wave is finally calculated.

PACS number(s): 52.40.Nk, 52.20.Dq, 52.60.+h, 03.30.+p

I. INTRODUCTION

Recently, the plasma physics involved in the interaction of a high-intensity laser beam with matter crossed the frontier which separates the classical plasmas from the so-called relativistic plasmas. In contrast to the usual terminology used in astrophysics, the term "relativistic" here means the high velocity, close to the light velocity c in vacuum, that the electrons of the medium irradiated by a focused laser beam may reach. This velocity is not isotropic but, *a priori,* in a plane normal to the propagation direction of the laser light and containing the incident-wave electric field. Recent compact lasers can produce 1-TW beams at (sub-) micrometer wavelengths which, after focusing, provide irradiance exceeding [1] 10^{18} W/cm^2, and make electrons in the focal volume oscillate with relativistic velocities. Indeed, the electron momentum, normalized to $m_e c$, can be written as $a_0=0.85\sqrt{I_0\lambda_0^2/10^{18}}$, where m_e denotes the electron mass, λ_0 is the laser wavelength in μm, and I_0 is the laser irradiance in W/cm^2. In addition to this transverse motion, another motion takes place along the propagation direction via the so-called ponderomotive force produced by the time-averaged laser energy gradient. As the ion mass makes the ions quasi-immobile, a restoring force tends to act on the mobile electrons, inducing an oscillating behavior. The electrons may then have a collective longitudinal motion with relativistic velocities, which gives rise to a very-high-amplitude electron plasma wave, an example of which can be found in the so-called wake-field effect [2].

It is easy to show that the longitudinal electron motion can be explained by the potential-energy profiles $|x|$ or x^2, where x denotes the space coordinate of the motion. Indeed, let us consider a semi-infinite homogeneous plasma with a vacuum/plasma interface at $x=0$. If, at equilibrium, the plasma is assumed to be constituted by immobile electrons and ions ensuring charge neutrality, the electron and ion density is given by $n_e=n_0 Y(x)$, where Y denotes the Heaviside function defined by $Y(x<0)=0$ and $Y(x\geq 0)=1$. We now analyze the evolution of the displacement of an electron slab around its equilibrium position x_{e0}. If the ions are assumed to remain immobile, Poisson's law gives the following electric field:

$$\frac{dE}{dx}=\frac{e}{\varepsilon_0}[n_0 Y(x)-n(x)]\ , \tag{1}$$

where $E(x)$ and $n(x)$ are the electric field and the electron density at location x, respectively; $-e$ is the electron charge; and ε_0 is the dielectric constant of vacuum. If no electron orbit crossing is assumed, the total negative charge located on each side of the electron location x is the same as for x_{e0}; only the ion positive charge is modified by the electron motion. As a result, Eq. (1) leads to the electric field $E(x)=n_0 e/\varepsilon_0[xY(x)-x_{e0}]$. We then obtain the potential energy of the electron as a function of its displacement: $-e\phi(x\geq 0)=m_e\omega_{pe}^2(x-x_{e0})^2/2$ and $-e\phi(x<0)=m_e\omega_{pe}^2 x_{e0}(x+x_{e0}/2)$, where ϕ is the electric potential and ω_{pe} is the electron plasma frequency $\sqrt{n_0 e^2/m_e\varepsilon_0}$. Therefore, depending on the electron position, a linear- or quadratic-shaped potential energy can drive the electron motion. Because the potential energy increases with $|x|$, without any limit, the electron is always trapped inside the potential well, regardless of its initial position or energy, result-

ing in a periodic motion. It should be noted that both these potential-energy expressions refer to a homogeneous density plasma or vacuum. Potential-energy expressions $K|x|^n$ with $n \geq 3$ correspond to situations where the plasma density is inhomogeneous with a profile symmetric at $x=0$.

Let us consider the specific sinusoidal potential. It refers to the motion of an electron which does not contribute to the collective effect; instead the electron feels the potential of an electron plasma wave induced by the harmonic motion of the plasma electrons oscillating in the above-mentioned quadratic potential. The sinusoidal potential is readily obtained when the electron motion in the collective effect is classical, i.e., with velocity $v \ll c$. As the potential energy oscillates between two finite limits, two kinds of particles may appear: the trapped particles, which remain inside one of the wells of the periodic pattern, and the untrapped particles, which may migrate over the whole pattern; the latter are high-energy particles in the wave frame. The trapped particle motion models the acceleration of an electron inside an electron plasma wave and is connected with the new concepts of plasma-based accelerators that use wake-field [2] and beat-wave [3–5] effects. The theoretical aspects of both of these effects have been covered at length [2,3]. Experimental evidence of large electric fields of a few GV/m have been obtained for beat wave only [4]. As to electron acceleration, only one experiment has so far demonstrated the acceleration of injected 2-MeV electrons to energies up to 9 MeV [5].

Whereas transverse and longitudinal motions along orthogonal directions are decoupled in the classical regime, they become coupled through the Lorentz factor in the particle momentum when velocities become relativistic. If the incident laser wave is assumed to be a plane wave with circular polarization, the transverse momentum $p_\perp$ is constant and equal to $|qA|$, where A denotes the wave-potential modulus and q is the particle charge. If $v_\perp$ denotes the velocity component of the particle in the transverse plane normal to the x axis, and v the particle velocity along the x axis, the Lorentz factor defined by $\gamma = 1/\sqrt{1-(v^2+v_\perp^2)/c^2}$ can also be written

$$\gamma = \frac{\gamma_\perp}{\sqrt{1-v^2/c^2}} , \tag{2}$$

where $\gamma_\perp$ is the transverse factor $\sqrt{1+(p_\perp/mc)^2}$, and m is the particle mass. Since $\gamma_\perp$ is constant for a circularly polarized wave, the transverse motion modifies the particle motion only along the x axis by increasing the electron mass by the factor $\gamma_\perp$, which enables us to isolate the particle motion along the x axis.

The undamped particle motion is described by the conservation of the Hamiltonian H, composed of the kinetic and potential energies:

$$H(x,v) = \frac{m\gamma_\perp c^2}{\sqrt{1-v^2/c^2}} + E_p(x) . \tag{3}$$

Without any loss of generality, we assume henceforth that the particle is initially located at the point that minimizes the potential energy; this location is defined as $x=0$, and we choose $E_p(0)=0$. If $\Phi(x)$ denotes the normalized potential energy $E_p(x)/m\gamma_\perp c^2$, and if we define $\gamma_{x0} = 1/\sqrt{1-v_0^2/c^2}$ as the initial "longitudinal" Lorentz factor, Eq. (3) becomes

$$\frac{1}{\sqrt{1-v^2/c^2}} + \Phi = \gamma_{x0} . \tag{4}$$

The basin shape of the potential energy around $x=0$ leads to the force $-\partial\Phi/\partial x$ with opposite sign with respect to x; this force tends to bring the particle toward the equilibrium position $(x,v)=(0,0)$, and then induces a periodic motion. The maximum particle momentum along the x axis is

$$p_{\max}/m\gamma_\perp c = \sqrt{\gamma_{x0}^2-1} . \tag{5}$$

Within a relativistic mechanics framework, previous analytical works [6,7] dealt with the quadratic potential energy only. In this paper, we first consider a more general algebraic expression for the potential energy, namely a power-law function of space, and, second, we examine a sinusoidal potential energy which is the most basic shape for any spatially periodic potential. Since the particle location and momentum can be expressed as functions of the potential energy Φ, a full understanding of the particle trajectory will depend on the ability to obtain some expression of the time as a function of the same parameter Φ. It should be noted that the results we obtained describe both single-particle motion and charged fluid slab motion. The latter is considered within a Lagrangian description in the context of no slab crossing, which enables us to model the charge behavior by a single-fluid model.

The paper is organized as follows. In Sec. II, the potential-energy profile $K|x|^n$ is considered, where K is a constant and n is a positive real number. In Sec. II A, we calculate the oscillation period in the general relativistic case and then give the expression for the weakly relativistic case. In Sec. II B, we specifically study the motion period for the cases $n=1$ and 2. In Sec. II C, the trajectory of the particle is given for both cases $n=1$ and 2. Section III is devoted to the sinusoidal potential energy. Section III A is concerned with the oscillation period; Sec. III B deals with the particle trajectory; and Sec. III C discusses the acceleration length of a particle in a fast-moving potential well. Conclusions are given in Sec. IV.

II. MOTION IN A POTENTIAL WELL $|x|^n$ WITH $n \geq 0$

The type of unbounded potential energy that we examine here leads to a finite range of particle excursion. The particle is trapped between the locations $-x_m$ and x_m, where the potential energy is at maximum: $\Phi_m = \gamma_{x0}-1$. The time can be expressed as a function of x or Φ by writing $t = \int_0^x dx'/v$. The tractability of our calculation is based on the use of the potential energy Φ as a new variable. The relation $\Phi = K|x|^n/m\gamma_\perp c^2$ leads, after some algebra, to the expression of time as a function of the potential energy:

$$t(\Phi)=\frac{|x_m|}{c}\frac{1}{\Phi_m^{1/n}n}\times\int_0^{\Phi}\frac{1+\Phi_m-\Phi'}{\Phi'^{(1-1/n)}\sqrt{(\Phi_m-\Phi')(2+\Phi_m-\Phi')}}d\Phi' \tag{6}$$

where the term on the right-hand side of the above expression has units of time. This integral needs to be rewritten in order to find some reference functions. For this purpose, we define $\psi=\Phi/\Phi_m$, so that ψ ranges from 0 to 1, and we define $z^2=\Phi_m/(2+\Phi_m)$, so that the expression for time becomes

$$t(\psi)=\frac{|x_m|}{c}\frac{1}{\sqrt{\Phi_m}}\left[\sqrt{2+\Phi_m}I_n(\psi)-\frac{1}{\sqrt{2+\Phi_m}}J_n(\psi)\right], \tag{7}$$

with

$$I_n(\psi)=\frac{1}{n}\int_0^{\psi}\psi'^{(1/n-1)}\frac{\sqrt{1-z^2\psi'}}{\sqrt{1-\psi'}}d\psi'$$

and

$$J_n(\psi)=\frac{1}{n}\int_0^{\psi}\psi'^{(1/n-1)}\frac{1}{\sqrt{1-z^2\psi'}\sqrt{1-\psi'}}d\psi' .$$

The constant which appears in front of the brackets in Eq. (7) is related to both the potential-energy shape and the particle excursion; the latter dependence disappears for the specific case $n=2$.

Now, by defining $\eta=\psi'/\psi$ and $u=\sqrt{\psi}(0<u<1)$, we can write the above integrals as hypergeometric functions of two variables, namely u^2 and u^2z^2, according to Gradhshteyn and Ryzhik's notation [8]:

$$I_n(u^2)=u^{2/n}{}_3F_1\left[\frac{1}{n},\frac{1}{2},-\frac{1}{2};1+\frac{1}{n};u^2,z^2u^2\right], \tag{8}$$

$$J_n(u^2)=u^{2/n}{}_3F_1\left[\frac{1}{n},\frac{1}{2},+\frac{1}{2};1+\frac{1}{n};u^2,z^2u^2\right], \tag{9}$$

where the function ${}_3F_1$ is given by

$${}_3F_1(\lambda,\mu,\nu;\sigma;p^2,q^2)=\frac{1}{B(\lambda,\sigma-\lambda)}\int_0^1\eta^{\lambda-1}(1-\eta)^{\sigma-\lambda-1}\times(1-p^2\eta)^{-\mu}(1-q^2\eta)^{-\nu}d\eta . \tag{10}$$

B denotes the beta function:

$$B(\lambda,\mu)=\int_0^1\eta^{\lambda-1}(1-\eta)^{\mu-1}d\eta=\frac{\Gamma(\lambda)\Gamma(\mu)}{\Gamma(\lambda+\mu)} , \tag{11}$$

where Γ is the Euler gamma function [8].

Equation (7) together with Eqs. (8) and (9) give time as a function of tabulated special functions and therefore close the set of equations which fully describes the particle trajectory. In Sec. II A, we focus on the period of motion and then examine in detail the trajectories for both the linear and quadratic potential shapes. We endeavored to scrupulously keep the notations and the order of the parameters for the special functions involved in the calculations.

A. Period of the oscillatory motion

At $x=0$, the potential energy is zero, i.e., $\psi=0$, and the kinetic energy is at a maximum, whereas at $x=x_m$ we have $\psi=1$ and the kinetic energy becomes zero. Therefore, the period for a full oscillation is simply written as $T_n=4t(1)$; that, is by using Eq. (7),

$$T_n=4\frac{|x_m|}{c}\frac{1}{\sqrt{\Phi_m}}\left[\sqrt{2+\Phi_m}I_n(1)-\frac{1}{\sqrt{2+\Phi_m}}J_n(1)\right] . \tag{12}$$

The expressions for $I_n(1)$ and $J_n(1)$ in Eqs. (8) and (9) can now be expressed as

$$I_n(1)=\frac{1}{n}B\left[\frac{1}{n},\frac{1}{2}\right]{}_2F_1\left[\frac{1}{n},-\frac{1}{2},\frac{1}{2}+\frac{1}{n},z^2\right], \tag{13}$$

$$J_n(1)=\frac{1}{n}B\left[\frac{1}{n},\frac{1}{2}\right]{}_2F_1\left[\frac{1}{n},\frac{1}{2},\frac{1}{2}+\frac{1}{n},z^2\right], \tag{14}$$

where ${}_2F_1$ denotes the following hypergeometric function for the single variable q^2:

$${}_2F_1(\lambda,\mu;\sigma;q^2)=\frac{1}{B(\lambda,\sigma-\lambda)}\times\int_0^1\eta^{\lambda-1}(1-\eta)^{\sigma-\lambda-1}(1-q^2\eta)^{-\mu}d\eta . \tag{15}$$

By using the equality $\Gamma(\frac{1}{2})=\sqrt{\pi}$ and Eq. (11), the general expression for the period becomes

$$T_n=4\sqrt{\pi}\frac{|x_m|}{c}\frac{1}{\sqrt{\Phi_m}}\frac{\Gamma\left[\frac{1}{n}\right]}{n\Gamma\left[\frac{1}{n}+\frac{1}{2}\right]}\times\left[\sqrt{2+\Phi_m}\,{}_2F_1\left[\frac{1}{n},-\frac{1}{2},\frac{1}{2}+\frac{1}{n},z^2\right]-\frac{1}{\sqrt{2+\Phi_m}}{}_2F_1\left[\frac{1}{n},\frac{1}{2},\frac{1}{2}+\frac{1}{n},z^2\right]\right] . \tag{16}$$

Figure 1 displays the surface $cT_n/|x_m|$ as a function of the potential exponent n and the maximum potential energy Φ_m; this plot has been drawn from tabulated functions obtained from software of Ref. [9]. We observe that T_n is a monotonically decreasing function of both parameters n and Φ_m, and that for $n\to 0$ and/or $\Phi_m\to 0$ the period exhibits a sharp increase. When $n\to 0$, the potential-energy profile is characterized by an increase around $x=0$ and a plateau for larger values of x, which become more and more localized and extended, respectively. Under such conditions, the particle that is initially located at $x=0$ loses its initial kinetic energy over a

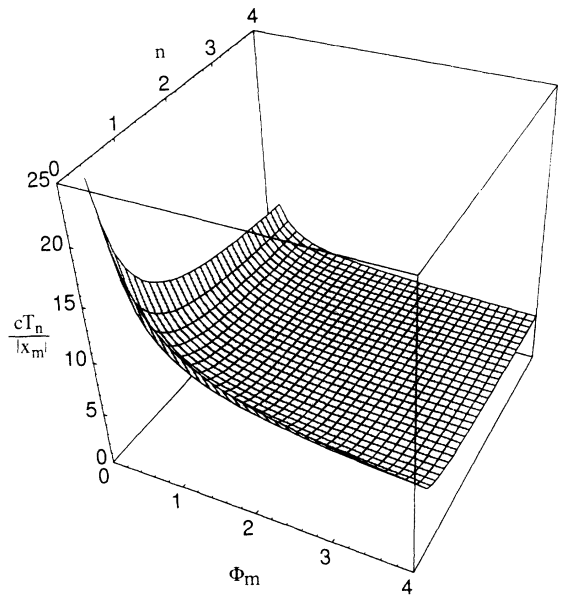

FIG. 1. Potential energy $K|x|^n$: period T_n as a function of the potential exponent n and the maximum potential energy Φ_m. T_n is referred to $|x_m|/c$, where x_m denotes the particle excursion.

short distance to reach the potential-energy plateau and then spends a long time at a slow velocity to reach the point x_m. This explains why the period of motion is increased by decreasing the potential exponent. Conversely, for $n \to \infty$, the potential-energy profile exhibits a plateau at larger and larger values and a sharp increase by approaching x_m. The period then can be found easily by considering the particle velocity v to be constant during the whole trajectory, with its value inferred from the energy conservation equality $\gamma_{x0}=1+\Phi_m$. The period is readily found to be $T_n=4|x_m|/v$, which takes the form $T_n=4|x_m|/c(1+\Phi_m)/\sqrt{\Phi_m(2+\Phi_m)}$. In the classical regime defined by $\Phi_m \ll 1$, we find $T_n=4|x_m|/c\,1/\sqrt{\Phi_m}$. Conversely, in the hyper-relativistic case, i.e., $\Phi_m \to \infty$, the period becomes $T_n=4|x_m|/c$, which is independent of n; this feature can be observed in Fig. 1.

We now consider the limit of a weakly relativistic motion, by assuming that the maximum potential energy is much lower than $m\gamma_\perp c^2$, so that z^2 is small compared to unity in the above expressions. In Eq. (7), the expansion to first order in z^2 of the integrals $I_n(1)$ and $J_n(1)$ leads to

$$B\left[\frac{1}{n},\frac{1}{2}\right] \pm \frac{z^2}{2} B\left[\frac{1}{n}+1,\frac{1}{2}\right], \tag{17}$$

where the signs + and − correspond to $I_n(1)$ and $J_n(1)$, respectively. After some algebra and by defining $A=\Gamma(1/n+1)\Gamma(1/n+\frac{1}{2})/[\Gamma(1/n+\frac{3}{2})\Gamma(1/n)]$ and retaining the terms to first order in Φ_m, we obtain the following expression for the period:

$$T_n=2\sqrt{\pi}\frac{|x_m|}{c}\frac{1}{\sqrt{\Phi_m}}\frac{\Gamma\left[\frac{1}{n}\right]}{n\Gamma\left[\frac{1}{n}+\frac{1}{2}\right]}\left[1+\tfrac{3}{4}\Phi_m(1-A)\right]. \tag{18}$$

In the so-called classical limit, i.e., $\Phi_m \to 0$, the general period becomes

$$T_n^c=2\sqrt{\pi}\frac{|x_m|}{c}\frac{1}{\sqrt{\Phi_m}}\frac{\Gamma\left[\frac{1}{n}\right]}{n\Gamma\left[\frac{1}{n}+\frac{1}{2}\right]}. \tag{19}$$

If, in addition, we assume $\gamma_\perp=1$, we are left with the equality

$$T_n^c=\frac{2\sqrt{2\pi m}}{K^{1/n}}\frac{\Gamma\left[\frac{1}{n}\right]}{n\Gamma\left[\frac{1}{n}+\frac{1}{2}\right]}\mathcal{E}^{1/n-1/2} \tag{20}$$

in which the second expression is exactly the classical result given in Ref. [10] if $\mathcal{E}$ denotes the initial kinetic energy $mc^2(\gamma_{x0}-1)$.

B. Oscillation period for the potential-energy shapes $|x|$ and x^2

In this section, we concentrate on the special cases $n=1$ and 2, which are usually relevant for laser-plasma interaction.

For the case $n=1$, Eqs. (8) and (9) give a simple relation, between I_1 and J_1:

$$I_1(1)=2_2F_1(1,-\tfrac{1}{2},\tfrac{3}{2},z^2)=\frac{1-z^2}{2}J_1(1)+1. \tag{21}$$

The resulting period for the linear potential is found to be

$$T_1=4\frac{|x_m|}{c}\left[\frac{2}{\Phi_m}+1\right]^{1/2}. \tag{22}$$

In the highly relativistic regime defined by $\Phi_m \gg 1$, the period decreases to the limit $T_1'=4|x_m|/c$ previously discussed. For the weakly relativistic motion, i.e., $\Phi_m \ll 1$. T_1 can be written from Eq. (22):

$$T_1=4\sqrt{2}\frac{|x_m|}{c}\frac{1}{\sqrt{\Phi_m}}(1+\tfrac{1}{4}\Phi_m). \tag{23}$$

For the classical motion limit, T_1 reduces to the following expression by using the potential strength K:

$$T_1^c=4\sqrt{2}\left[\frac{|m|x_m|}{K}\right]^{1/2}. \tag{24}$$

To make a connection to a plasma, where K is written as $m_e\omega_{pe}^2 x_{e0}/\gamma_\perp$, with x_{e0} the electron position referred to the plasma edge as defined in Sec. I, the period above can

be written as $\omega_{pe}T_1^c=4\sqrt{2}\sqrt{\gamma_\perp x_m/x_{e0}}$.

For the case $N=2$, after using $B(1/2,1/2)=\pi$ Eqs. (13)–(15) become:

$$I_2(\psi)=E\left[\frac{\pi}{2},z\right],\quad J_2(\psi)=F\left[\frac{\pi}{2},z\right], \tag{25}$$

where F and E denote complete elliptic integrals of the first and second kinds with argument $\pi/2$ and modulus z, according to definitions in Ref. [8]. Equation (8) leads to the following period:

$$T_2=4\frac{|x_m|}{c}\frac{1}{\sqrt{\Phi_m}}\left[\sqrt{2+\Phi_m}E\left[\frac{\pi}{2},z\right]-\frac{1}{\sqrt{2+\Phi_m}}F\left[\frac{\pi}{2},z\right]\right], \tag{26}$$

where the constant in front of the brackets does not actually depend on x_m but only on the potential strength K, in contrast to the period T_1, and more generally with any period T_n when $n\neq 2$. The above expression recovers exactly the expression put forward in MacColl's paper [7]. Figure 1 shows that, as a function of Φ_m, the curve of T_2 always lies below the curve for T_1. For the weakly relativistic case defined by $\Phi_m \ll 1$, the elliptic integrals expand according to $E(\pi/2,z)=\pi/2(1-z^2/4)$ and $F(\pi/2,z)=\pi/2(1+z^2/4)$; the resulting period becomes, to first order in Φ_m,

$$T_2=\sqrt{2}\pi\frac{|x_m|}{c}\frac{1}{\sqrt{\Phi_m}}(1+\tfrac{3}{8}\Phi_m)\,. \tag{27}$$

By using the potential strength K, the classical motion limit is characterized by the following period:

$$T_2^c=\pi\left[\frac{2m}{K}\right]^{1/2}. \tag{28}$$

In a plasma, where $K=m_e\omega_{pe}^2/2\gamma_\perp$, the above period has the usual expression $T_2^c=2\pi\sqrt{\gamma_\perp}/\omega_{pe}$. Also, Eq. (27) provides the correction to the plasma frequency for $\gamma_\perp=1$:

$$\omega_2=\omega_{pe}\left[1-\frac{3}{16}\left[\frac{\omega_{pe}}{c}\right]^2 x_m^2\right], \tag{29}$$

in agreement with the standard expression found in Ref. [11].

C. Particle trajectory for $n=1$ and 2

The particle position and momentum can be obtained as functions of time through parametric expressions in which the normalized potential energy $\psi=\Phi/\Phi_m$ is the parameter; the latter ranges from 0 to 1.

For $n=1$, the motion is characterized by the following parametric equations:

$$\begin{aligned} t(\psi)&=\frac{|x_m|}{c}\frac{1}{\sqrt{\Phi_m}}\sqrt{2+\Phi_m}[1-\sqrt{(1-\psi)(1-z^2\psi)}]\,,\\ x(\psi)&=x_m\psi\,,\\ \frac{p(\psi)}{m\gamma_\perp c}&=\sqrt{(1+\Phi_m(1-\psi))^2-1}\,, \end{aligned} \tag{30}$$

with $|x_m|=(\gamma_{x0}-1)/K$. The first equation is derived from Eq. (7), the second from the definition of ψ, and the last one from the conservation of the Hamiltonian in Eq. (3). For $\psi=0$, we recover the initial conditions $t=0$, $x=0$, and $p/m\gamma_\perp c=\sqrt{\gamma_{x0}^2-1}$. The value $\psi=1$ gives $t=T_1/4$, $x=x_m$, and $p=0$; these values are related to the extremum of the particle position. Actually, the expression $t(\psi)$ can be inverted into $\psi(t)$, such that the trajectory can be obtained explicitly as a function of time:

$$\frac{x(t)}{x_m}=\frac{1}{\Phi_m}\left\{(1+\Phi_m)-\left[(1+\Phi_m)^2+4\Phi_m^{3/2}\frac{c}{|x_m|}t\left[\sqrt{\Phi_m}\frac{c}{|x_m|}t-2\sqrt{2+\Phi_m}\right]\right]^{1/2}\right\}. \tag{31}$$

Orbits $x(t)$ and momentum $p(t)$ are displayed in Figs. 2 and 3, respectively, for various values of Φ_m. The evolution of the phase diagram as a function of Φ_m is shown in Fig. 4. The period decrease with increasing Φ_m can be seen clearly. The momentum dependence with respect to time has a triangular shape, which indicates a uniformly accelerated motion.

In the classical regime, we can expand x and p as functions of Φ_m to obtain the following expressions for both position and velocity:

$$\begin{aligned} \frac{x(t)}{x_m}&=\left[\frac{\Phi_m}{2}\right]^{1/2}\frac{c}{|x_m|}t\left[2-\left[\frac{\Phi_m}{2}\right]^{1/2}\frac{c}{|x_m|}t\right],\\ \frac{v(t)}{c}&=\sqrt{2\Phi_m}-\Phi_m\frac{c}{|x_m|}t\,. \end{aligned} \tag{32}$$

The position is a quadratic function of time, which is also the usual specific feature of a uniformly accelerated classical motion. The pattern exhibited by these expressions can be recovered from Figs. 2 and 3, for $\Phi_m=0.1$.

For $n=2$, the parametric expressions for time, position, and momentum, respectively, are written

$$\begin{aligned} t(\lambda)&=\frac{|x_m|}{c}\frac{1}{\sqrt{\Phi_m}}\left[\sqrt{2+\Phi_m}E(\lambda,z)-\frac{1}{\sqrt{2+\Phi_m}}F(\lambda,z)\right],\\ x(\lambda)&=x_m\sin(\lambda)\,,\\ \frac{p(\lambda)}{m\gamma_\perp c}&=\sqrt{\{1+\Phi_m[1-\sin^2(\lambda)]\}^2-1}\,, \end{aligned} \tag{33}$$

where λ is defined by the expression $\lambda=\sin^{-1}\sqrt{\psi}$. As for the velocity expression, we find

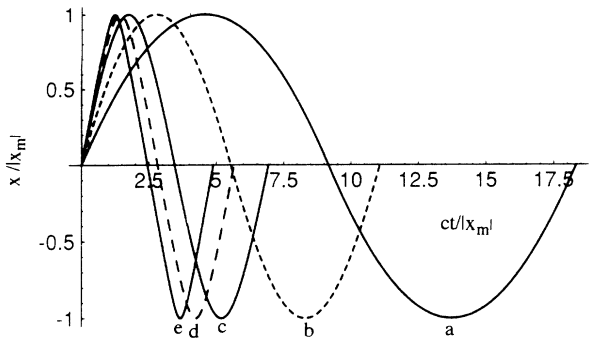

FIG. 2. Potential energy $K|x|$: particle location x as a function of time for various maximum potential energies Φ_m: (a) 0.1, (b) 0.3, (c) 1, (d) 2, and (e) 4. At $t=0$, the particle is located at $x=0$ with the Lorentz factor $\gamma_{x0}=1+\Phi_m$. Time is referred to $|x_m|/c$, where x_m denotes the particle excursion.

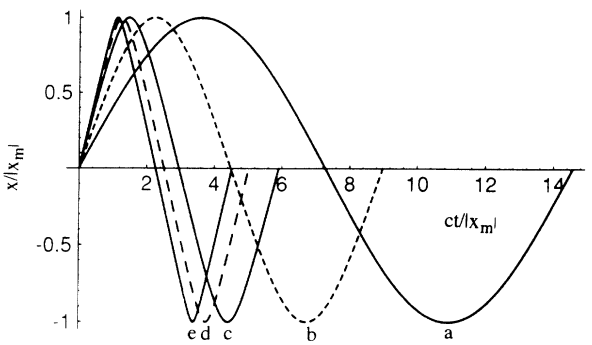

FIG. 5. Potential energy Kx^2: particle location as a function of time for various maximum potential energies Φ_m: (a) 0.1, (b) 0.3, (c) 1, (d) 2, and (e) 4. At $t=0$, the particle is located at $x=0$ with the Lorentz factor $\gamma_{x0}=1+\Phi_m$. Time is referred to $|x_m|/c$, where x_m denotes the particle excursion.

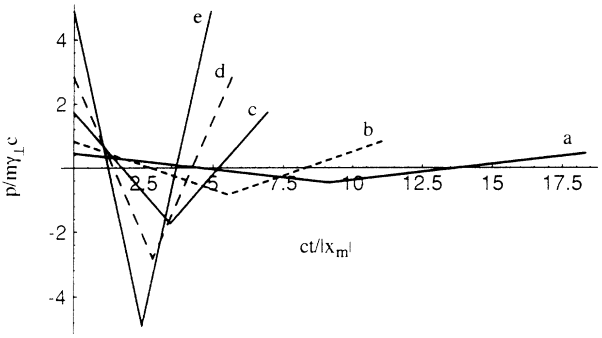

FIG. 3. Potential energy $K|x|$: particle momentum $p/m\gamma_\perp c$ along the x axis as a function of time for various maximum potential energies Φ_m: (a) 0.1, (b) 0.3, (c) 1, (d) 2, and (e) 4. At $t=0$, the particle is located at $x=0$ with the Lorentz factor $\gamma_{x0}=1+\Phi_m$. Time is referred to $|x_m|/c$, where x_m denotes the particle excursion.

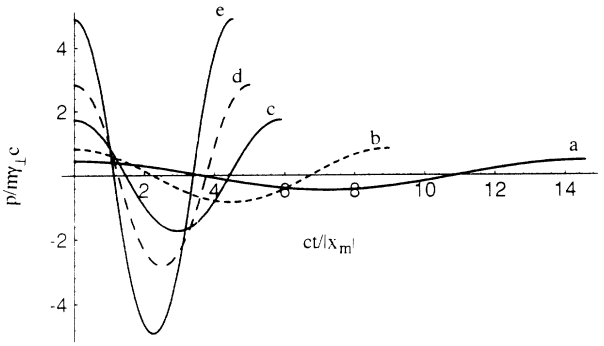

FIG. 6. Potential energy Kx^2: particle momentum $p/m\gamma_\perp c$ as a function of time for various maximum potential energies Φ_m: (a) 0.1, (b) 0.3, (c) 1, (d) 2, and (e) 4. At $t=0$, the particle is located at $x=0$ with the Lorentz factor $\gamma_{x0}=1+\Phi_m$. Time is referred to $|x_m|/c$, where x_m denotes the particle excursion.

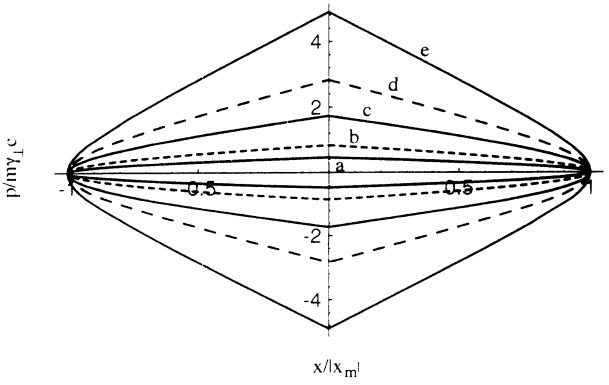

FIG. 4. Potential energy $K|x|$: phase space (location x referred to the particle excursion x_m, momentum $p/m\gamma_\perp c$) for various maximum potential energies Φ_m: (a) 0.1, (b) 0.3, (c) 1, (d) 2, and (e) 4. As a function of time, a particle follows the contours in a clockwise direction.

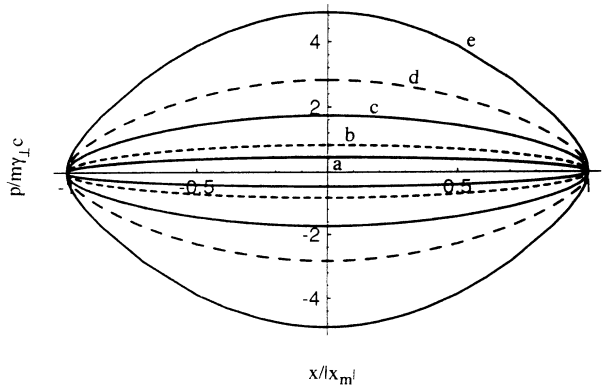

FIG. 7. Potential energy Kx^2: phase space (location x referred to the particle excursion x_m, momentum $p/m\gamma_\perp c$), for various maximum potential energies Φ_m: (a) 0.1, (b) 0.3, (c) 1, (d) 2, and (e) 4.

$$\frac{v(\lambda)}{c}=\sqrt{\Phi_m}\frac{\sqrt{2+\Phi_m\cos^2(\lambda)}\cos(\lambda)}{1+\Phi_m\cos^2(\lambda)} . \tag{34}$$

By defining parameter λ, the time is written as a function of the elliptic integrals, which clearly shows the motion period. When $\psi=0$, which yields $\lambda=0$, we get the initial conditions $t=0$, $x=0$, and $p=p_{\max}$ given by Eq. (5). At the top excursion of the potential well, when $\psi=1$, we have $\lambda=\pi/2$, so that the expressions give $t=T_2/4$, where T_2 is the complete period of the motion defined in Eq. (26), $x=x_m$, and $p=0$. The trajectory $x(t)$ and momentum $p(t)$ are displayed in Figs. 5 and 6, respectively, for various values of Φ_m; the phase diagram (x,p) associated with the motion is displayed in Fig. 7.

In the classical regime $\Phi_m\to 0$, from the combination of expressions (33) we can infer the usual expression for the position and velocity:

$$x(t)=x_m\cos(\omega_2 t) ,$$
$$\frac{v(t)}{c}=\sqrt{2\Phi_m}\sin(\omega_2 t) , \tag{35}$$

where $\omega_2=\sqrt{2K/m}$. In Figs. 5–7, the classical case corresponds to the value $\Phi_m=0.1$.

III. MOTION IN A cos(x) POTENTIAL

The normalized potential energy is written as $\Phi(x)=\varepsilon[1-\cos(kx)]$, where k denotes the wave vector of the periodic pattern. With this choice, the equilibrium point is kept at $(x,v)=(0,0)$ as in Sec. II. A major difference from Sec. II is that the potential energy has a finite maximum bounded by 2ε. This means that a particle can either be trapped and oscillate in the potential well (the orbit stays in a finite extension domain) or be untrapped and keep a constant velocity sign (the orbit explores an unlimited-extension space). The particle is located initially at $x=0$, where the potential is zero, with the "longitudinal" Lorentz factor γ_{x0}. The trapping region corresponds to the Lorentz factor domain located below the separatrix line whose equation is written

$$\gamma_{x0}\le 1+2\varepsilon . \tag{36}$$

The untrapping region is associated with the opposite condition.

As before, we obtain the time as a function of the location from the relation $t=\int_0^x dx/v$, and by the energy conservation Eq. (4) rewritten as

$$\frac{1}{\sqrt{1-(dx/cdt)^2}}=\gamma_{x0}-\Phi . \tag{37}$$

By using the notation $\Phi_m=\gamma_{x0}-1$, we obtain the following expression of time as a function of the potential energy Φ:

$$t(\Phi)=\frac{1}{kc}\left[\int_0^{\Phi}\left[\frac{2+\Phi_m-\Phi'}{\Phi'(\Phi_m-\Phi')(2\varepsilon-\Phi')}d\Phi'\right]^{1/2}-\int_0^{\Phi}\frac{d\Phi'}{\sqrt{(2+\Phi_m-\Phi')\Phi'(\Phi_m-\Phi')(2\varepsilon-\Phi')}}\right] . \tag{38}$$

A. Oscillation period

First we consider the untrapped particle regime, i.e., $\gamma_{x0}>1+2\varepsilon$. The particle moves in the whole potential energy domain from 0 to 2ε. We can define the period of the motion as the time required by the particle to jump from the initial well bottom to the next bottom; thus the period can be written as $T_u=2t(2\varepsilon)$, where the subscript u stands for untrapped particles. In Eq. (38), the expression under the radical sign remains positive, so that there are no conditions on the solution. After some algebra, we find that both integrals in Eq. (38) can be written as functions of tabulated functions, so that the period T_u becomes

$$T_u=\frac{1}{kc}\frac{1}{\sqrt{\Phi_m(1+\Phi_m-\varepsilon)}}\times\left[2(1+\Phi_m)\Pi\left[\frac{\pi}{2},\frac{-\varepsilon}{1+\Phi_m-\varepsilon},r_u\right]-F\left[\frac{\pi}{2},r_u\right]\right] \tag{39}$$

where Π and F denote complete elliptic integrals of the third and first kinds, respectively, according to notations in Ref. [8] and where the expression of the modulus r_u is

$$r_u=\left[\frac{\varepsilon}{\Phi_m(1+\Phi_m-\varepsilon)}\right]^{1/2} . \tag{40}$$

We now consider the trapped particle motion. As the particle remains in a bounded domain, the period is four times the time needed by the particle to go from its initial position to its stopping point x_m. Clearly, as Φ_m remains lower than 2ε, the expression in the square roots involved in Eq. (38) are positive. From Ref. [8], the solution depends on the relative importance of 2ε and $2+\Phi_m$. Henceforward, case P will refer to the situation when the following inequality is fulfilled: $2\varepsilon\le 2+\Phi_m$, and case Q will refer to the opposite situation $2+\Phi_m\le 2\varepsilon$. It should be noted that in the classical regime, i.e., $\varepsilon\ll 1$, condition P is always fulfilled; in the hyper-relativistic regime, defined by $\varepsilon\gg 1$, the domain P is close to the separatrix and the trajectory is essentially inside the domain Q. From Ref. [8] we find the following periods:

$$T_P=\frac{4}{kc}\frac{1}{\sqrt{\varepsilon}}\left[(2+\Phi_m)\Pi\left[\frac{\pi}{2},-\frac{\Phi_m}{2},r_P\right]-F\left[\frac{\pi}{2},r_P\right]\right] , \tag{41}$$

$$T_Q=\frac{8}{kc}\frac{1}{\sqrt{(2\varepsilon-\Phi_m)(2+\Phi_m)}}\times\left[\varepsilon\Pi\left[\frac{\pi}{2},\frac{-\Phi_m}{2\varepsilon-\Phi_m},r_Q\right]-(2\varepsilon-\Phi_m-1)F\left[\frac{\pi}{2},r_Q\right]\right] , \tag{42}$$

where

$$r_P=\left[\frac{(2+\Phi_m-2\varepsilon)\Phi_m}{4\varepsilon}\right]^{1/2}$$

and

$$r_Q=\left[\frac{(2\varepsilon-2-\Phi_m)\Phi_m}{(2\varepsilon-\Phi_m)(2+\Phi_m)}\right]^{1/2}.$$

The period is continuous, i.e., $T_P=T_Q$, at $2+\Phi_m=2\varepsilon$, which is the boundary between domains P and Q. Actually, the expression for T_Q can be recovered exactly from Eq. (41) by replacing 2 by $2\varepsilon-\Phi_m$. The distinction between cases P and Q comes from the use of parameter r, which involves a square root; this distinction can be overlooked in plotting by using the elliptic functions available in Ref. [9], which use r^2 instead of r as an argument. Figure 8 displays the evolution of periods T_u and T_P as functions of E_m for various values of ε; E_m denotes the initial longitudinal kinetic energy $\gamma_{x0}-1$. The lowest value of $\varepsilon=0.1$ gives rise to low velocities and then to classical motion, whereas the highest value of ε leads to relativistic motion. The period decreases with $E_m/2\varepsilon$, as expected. When the particle energy approaches infinity, the particle velocity can be considered as constant and equal to c; the time to travel along one wavelength is simply $2\pi/kc$, which can be verified to be the right-hand limit in Fig. 8.

When the particle stays near the basin bottom at $x=0$, i.e., $kx\ll 1$, the potential energy has a simple quadratic dependence with respect to x: $\Phi(x)=\varepsilon(kx)^2/2$. It follows that the third-order elliptic integral Π in Eq. (41) reduces to a second-order elliptic integral; as a result, from the expression for T_P we recover the period associated with the quadratic potential energy given in Sec. II B with $K/m\gamma_\perp c^2=\varepsilon k^2/2$:

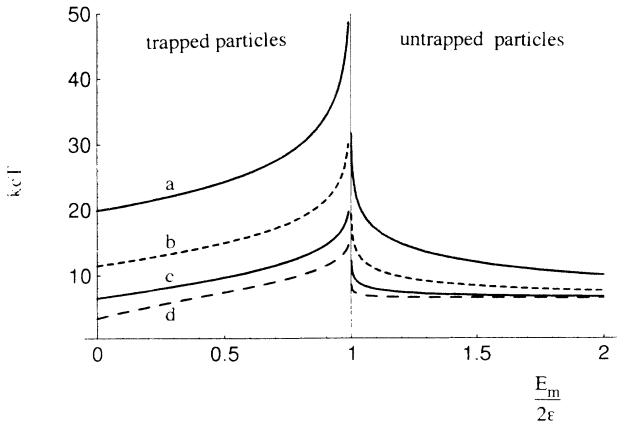

FIG. 8. Potential energy $\varepsilon[1-\cos(kx)]$: period as a function of the ratio of the maximum total particle energy E_m to the maximum well potential strength 2ε. The energy E_m is defined as $E_m=\gamma_{x0}-1+\Phi_m$. The potential energy strength ε is (a) 0.1, (b) 0.3, (c) 1, and (d) 4. The separatrix between trapped and untrapped particle domains is at $E_m/2\varepsilon=1$.

$$T_P=\frac{4}{kc}\left[\frac{2}{\varepsilon}\right]^{1/2}\left[\sqrt{2+\Phi_m}\,E\left[\frac{\pi}{2},z\right]-\frac{1}{\sqrt{2+\Phi_m}}F\left[\frac{\pi}{2},z\right]\right]. \tag{43}$$

In the weakly relativistic limit, which allows us to expand Eq. (43) to first order in Φ_m, the oscillation period becomes

$$T_P=\frac{4}{kc}\frac{1}{\sqrt{\varepsilon}}\left[F\left[\frac{\pi}{2},r_P\right]+\tfrac{3}{2}\varepsilon E\left[\frac{\pi}{2},r_P\right]-(2\varepsilon-\Phi_m)F\left[\frac{\pi}{2},r_P\right]\right], \tag{44}$$

where $r_P=\sqrt{\Phi_m/2\varepsilon}$. The limit $\Phi_m\to 0$ leads to the value $\pi/2$ for both elliptic integrals, which results in the classical limit $T_P=2\pi/(kc\sqrt{\varepsilon})$. For a plasma, we have $K=m_c\omega_{pe}^2/2\gamma_\perp$, so that the classical period reduces to the expression $2\pi\sqrt{\gamma_\perp}/\omega_{pe}$, which is the standard trapping period, except for the electron mass increase due to the transverse Lorentz factor.

B. Particle trajectory

We limit our analysis to the trapped particle. By using the parameter β_P defined by

$$\Phi=\frac{(2+\Phi_m)\Phi_m\sin^2(\beta_P)}{2+\Phi_m\sin^2(\beta_P)} \tag{45}$$

in Eq. (38), we obtain the following expressions of the time, location, and momentum:

$$t_P(\beta_P)=\frac{1}{kc}\frac{1}{\sqrt{\varepsilon}}\left[(2+\Phi_m)\Pi\left[\beta_P,-\frac{\Phi_m}{2},r_P\right]-F(\beta_P,r_P)\right], \tag{46}$$

$$kx_P(\beta_P)=\cos^{-1}\left[1-\frac{\Phi_m(2+\Phi_m)\sin^2(\beta_P)}{\varepsilon[2+\Phi_m\sin^2(\beta_P)]}\right], \tag{47}$$

$$\frac{p_P(\beta_P)}{m\gamma_\perp c}=\left[\left[\frac{2+2\Phi_m-\Phi_m\sin^2(\beta_P)}{2+\Phi_m\sin^2(\beta_P)}\right]^2-1\right]^{1/2}. \tag{48}$$

Equations (46)–(47) are correctly written for the condition $2+\Phi_m\geq 2\varepsilon$. When the opposite condition $2+\Phi_m\leq 2\varepsilon$ has to be considered, we have to change 2 to $2\varepsilon-\Phi_m$ to obtain the correct expressions. The initial condition $\Phi=0$ is recovered from Eqs. (45)–(48): since $\beta_P=0$, then $t=0$, $x=0$, and $p/m\gamma_\perp c=\sqrt{(1+\Phi_m)^2-1}$. For $\Phi=\Phi_m$, $\beta_P=\pi/2$, so that $t=T_P/4$, $kx=\cos^{-1}(1-\phi_m/\varepsilon)=kx_m$, and $p=0$; these conditions correspond to the position extremum of the particle.

Figures 9 and 10 show the position and momentum of a trapped particle as functions of time, and Fig. 11 displays the phase diagram (x,p) for a trapped particle. We have chosen the value $\varepsilon=2.5$; the maximum potential energy ranges from $\Phi_m/2\varepsilon=0.2$ to 0.975. We can ob-

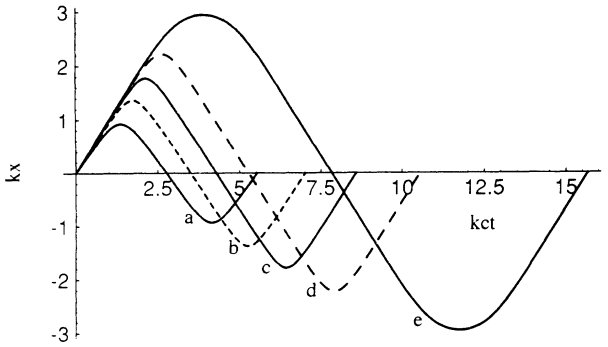

FIG. 9. Potential energy $\varepsilon[1-\cos(kx)]$: location of a trapped particle as a function of time (referred to as kc) for $\varepsilon=2.5$, and for the maximum potential $\Phi_m=$ (a) 1, (b) 2, (c) 3, (d) 4, and (e) 4.95. At $t=0$, the particle is at $x=0$, with the Lorentz factor $\gamma_{x0}=1+\Phi_m$.

serve that aspects of both trajectory and momentum change rapidly when approaching the separatrix at $\Phi_m \geq 1.95\varepsilon$, as compared to smaller values of Φ_m.

For the classical limit, i.e., $\varepsilon \ll 1$, β_P and r_P become $\sin^{-1}(\sqrt{\Phi/\Phi_m})$ and $\sqrt{\Phi_m/2\varepsilon}$, respectively. In Eq. (46), the third-order elliptic integral $\Pi(\beta_P,-\Phi_m/2,r_P)$ reduces to $F(\beta_P,r_P)$, giving the following expressions for the time and particle position and velocity as functions of the potential energy:

$$t_P(\Phi)=\frac{1}{kc}\frac{1}{\sqrt{\varepsilon}}F\left[\sin^{-1}\left[\frac{\Phi}{\Phi_m}\right]^{1/2},\left[\frac{\Phi_m}{2\varepsilon}\right]^{1/2}\right], \quad (49)$$

$$x_P(\Phi)=\frac{1}{k}\cos^{-1}\left[1-\frac{\Phi}{\varepsilon}\right], \quad (50)$$

$$\frac{v_P(\Phi)}{c}=\sqrt{2(\Phi_m-\Phi)}, \quad (51)$$

in agreement with the standard result reported in Ref. [10].

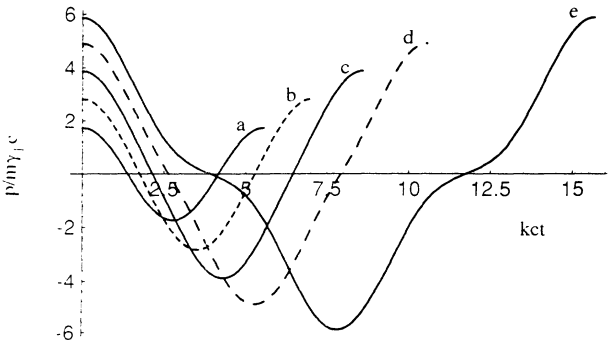

FIG. 10. Potential energy $\varepsilon[1-\cos(kx)]$: momentum $p/m\gamma_\perp c$ of a trapped particle as a function of time for $\varepsilon=2.5$ and the maximum potential $\Phi_m=$ (a) 1, (b) 2, (c) 3, (d) 4, and (e) 4.95. At $t=0$, the particle is at $x=0$, with the Lorentz factor $\gamma_{x0}=1+\Phi_m$.

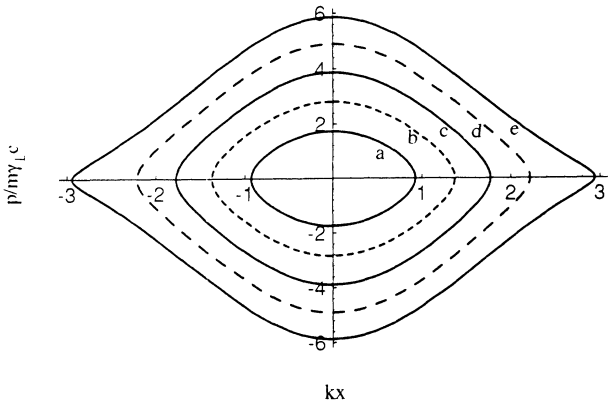

FIG. 11. Potential energy $\varepsilon[1-\cos(kx)]$: phase portrait (location x, momentum $p/m\gamma_\perp c$) of a trapped particle. We use $\varepsilon=2.5$; the values of the maximum potential are $\Phi_m=$ (a) 1, (b) 2, (c) 3, (d) 4, and (e) 4.95.

C. Particle acceleration length

In the previous sections, we have assumed that the potential well was immobile. If this well is associated with a wave with nonzero phase velocity, the above calculations have to be carried out in the rest frame of the wave and the quantities involved in the preceding equations transformed from the lab frame via a Lorentz transform. If v_ϕ denotes the phase velocity and γ_ϕ the phase Lorentz factor defined by $\gamma_\phi=1/\sqrt{1-v_\phi^2/c^2}$, then the electric field is $E_M\sin(k_L[x_L-v_\phi t_L)]$ in the lab frame and $E_M\sin(kx)$ with $k=k_L/\gamma_\phi$ in the wave frame (the subscript L stands for lab frame); as for the electric potential, we have, respectively, $\phi_{ML}\cos[k_L(x_L-v_\phi t_L)]$ and $\phi_M\cos(kx)$ with the relation $\phi_M=\gamma_\phi\phi_{ML}$. The space-time quadrivector modifies via the Lorentz relations to $t=\gamma_\phi(t_L-v_\phi x_L/c^2)$ and $x=\gamma_\phi(x_L-v_\phi t_L)$.

There are basically two physical problems associated with electron acceleration. On the one hand, we can look for the plasma length $l_{La}(\Phi_m)$ in the lab frame required for an electron located at Φ_m potential energy with zero velocity to go down to $\Phi=0$ where its kinetic energy maximizes; such a length is the so-called acceleration length. On the other hand, we can also look for the maximum energy represented by the Lorentz factor $\gamma_{ML}(l_L)$ that an electron can reach when the plasma length is imposed to be l_L in the lab frame. In the following, we shall concentrate on the first consideration.

We consider the initial condition $k_L x_{mL}=kx_m=-\cos^{-1}(1-\Phi_m/\varepsilon)$. Since the wave phase is conserved by a Lorentz transformation, at any time during the particle motion we have the equality $k_L(x_{mL}+l_L-v_\phi t_L)=kx=-\cos^{-1}(1-\Phi/\varepsilon)$, where l_L denotes the distance the particle propagates from x_m in the lab frame. The Lorentz relations lead to the following expression for the distance in the lab frame associated with the particle motion from the initial potential Φ_m to the potential energy Φ:

$$l_L=v_\phi\gamma_\phi[t(\Phi_m)-t(\Phi)]+\frac{1}{k_L}[\cos^{-1}(1-\Phi_m/\varepsilon)-\cos^{-1}(1-\Phi/\varepsilon)]. \quad (52)$$

The so-called acceleration length is defined by $\Phi=0$, so that we can write

$$l_{La}=v_\phi\gamma_\phi t(\Phi_m)+\frac{1}{k_L}\cos^{-1}(1-\Phi_m/\varepsilon)\ . \tag{53}$$

For a fixed wave, we recover the wave-frame result $k_L l_{La}=\cos^{-1}(1-\Phi_m/\varepsilon)$, i.e., a finite plasma length. The case $\Phi_m=2\varepsilon$ gives $k_L l_{La}=\pi$, which corresponds to half a wavelength. Conversely, if the phase velocity approaches the light velocity in vacuum, the acceleration length largely exceeds the wavelength, so that l_{La} becomes simply proportional to $t(0)$. We have a useful gauge for the acceleration length by assuming that the electric field is constant with value E during the particle acceleration, so that we can write $\Delta\Phi_L/2=qE/mc^2k_L$. The momentum increases according to $p=qEt$, which gives $\gamma_x\approx qEt/mc$ if $p/mc\gg-1$. Since the particle Lorentz factor can be written $\gamma_x=1+\gamma_\phi\Delta\Phi_L\approx\gamma_\phi\Delta\Phi_L$, we obtain an estimate of the acceleration length $l_{Le}=2ct_L\approx4\gamma_\phi^2/k_L$ by means of the time-space transformation.

Figure 12 displays the ratio l_{La}/γ_ϕ^2 given by Eq. (53) for potential strengths ε ranging from 0.1 to 4 in the lab frame and for $\gamma_\phi=10$. The increase of the potential energy by the Lorentz transformation from the lab frame to the wave frame gives rise to relativistic motion even for the lowest value $\varepsilon=0.1$. The time involved in Eq. (53) is given by Eq. (39). We observe that the estimate of the acceleration length corresponds to the critical point above which the length increases dramatically. The maximum energy 2ε requires an infinite time to reach and hence an infinite plasma length; this limit corresponds to $\Phi_m=2\varepsilon$ in Fig. 12 (the curves have been truncated by the plot process). The value l_{Le} is a correct estimate of the acceleration length since the particle energy gain is very close to Φ_m for this value. Figure 12 compares well with the result from Ref. [12] which reports numerical integration of the particle motion for the case $\gamma_\phi=10$. For $\varepsilon\to0$, the particle motion period diverges to infinity, so that the acceleration length itself becomes infinite. For a particle which is initially located close to the basin bottom, the period is $2\pi/(kc\sqrt{\varepsilon})$ in the wave frame, according to Sec. III B. If the $\cos^{-1}(\ )$ term is disregarded in Eq. (53), which is valid for $\gamma_\phi\gg1$, we obtain the acceleration $l_{La}=c\gamma_\phi\pi/(2\sqrt{\gamma_\phi\varepsilon})$. This length is larger than the estimate l_{Lc} for low values of ε, more precisely $\varepsilon<(\pi/8)^2/\gamma_0^3$.

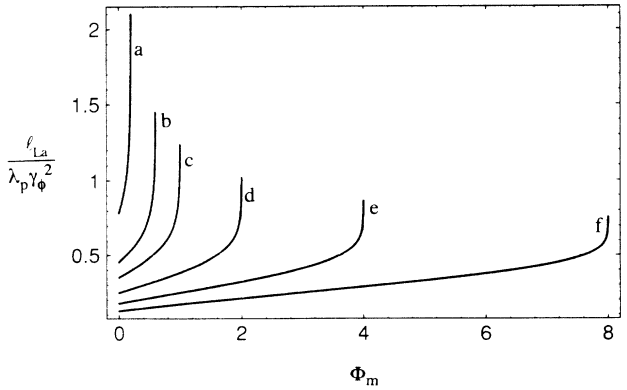

FIG. 12. Potential energy $\varepsilon[1-\cos(kx)]$: acceleration length $l_{La}/\gamma_\phi^2\lambda_p$ as a function of the maximum potential energy Φ_m; both quantities are given in the lab frame. The phase Lorentz factor is $\gamma_\phi=10$ and the potential strength in the lab frame is $\varepsilon=$(a) 0.1, (b) 0.3, (c) 0.5, (d) 1, (e) 2, and (f) 4. λ_p is the potential wavelength $2\pi/k_L$ in the lab fame.

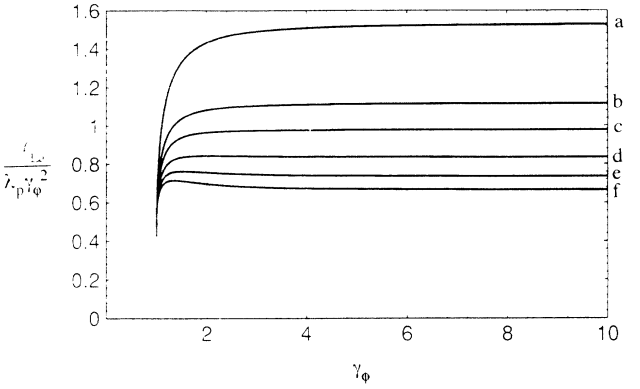

FIG. 13. Potential energy $\varepsilon[1-\cos(kx)]$: acceleration length $l_{La}/\gamma_\phi^2\lambda_p$ in the lab frame as a function of the phase Lorentz factor. The potential strength ε is (a) 0.1, (b) 0.3, (c) 0.5, (d) 1, (e) 2, and (f) 4 in the lab frame. The potential wavelength $\lambda_p=2\pi/k_L$ in the lab frame. For all plots, the particle is initially located at the same point in the potential well: $\Phi_m=2\varepsilon-0.01$.

Figure 13 shows the dependence of the acceleration length with respect to γ_ϕ, for various values of ε. The acceleration length decreases with increasing potential strength ε. For $\gamma_\phi=1$, all the curves converge to the same value $l_{La}=0.45\lambda_p$; the difference from $\lambda_p/2$ is caused by the initial particle location slightly below the potential top. When $\varepsilon\to\infty$, the acceleration length approaches the preceding estimate l_{Le}. This can be explained by the fact that the particle has a constant velocity equal to c and thus does not depend on the real potential-energy amplitude.

The problem related to the energy gain in a finite imposed plasma length can be solved using Eq. (52), which gives implicitly the potential energy Φ felt by the particle when the particle has transited along the distance l_L. The Lorentz factor of the particle is then $\gamma_x=1+\gamma_\phi\Delta\Phi_L$, which in the wave frame becomes

$$\gamma_{xL}=\gamma_\phi(1+\gamma_\phi\Delta\Phi_L)+\sqrt{\gamma_\phi^2-1}\sqrt{\gamma_\phi\Delta\Phi_L(\gamma_\phi\Delta\Phi_L+2)}\ . \tag{54}$$

IV. CONCLUSION

We summarize our work first. We have analytically examined the motion of a relativistic particle whose potential energy depends on x via a power-law expression $|x|^n$ or via a pure sinusoidal expression. Various figures have been included in this paper in order to shed light on the intricate expressions that underlie the particle

motion. We have also systematically discussed both the classical and hyper-relativistic limits, and we have tried to find some intuitive explanation for the analytical results. The expression for the period of the oscillatory motion was given for any value for n. The classical limit deduced from this general expression fully agrees with the usual result. The trajectories for the cases $n=1$ and 2 have been more extensively discussed because they are more relevant to laser-plasma interaction. For the sinusoidal potential, the period was calculated for both trapped and untrapped particles. The trajectories were also defined parametrically. The analytic expression for the acceleration length was given as a function of both the initial energy of the particle and the wave-phase velocity.

The analytical results which have been presented throughout this paper can be useful in various situations. They can be considered as a useful gauge when more complex potential-energy shapes are considered, such as those given by the wake-field concept. Furthermore, knowledge of both the period and the trajectory is useful to consider the radiation emitted by a plasma illuminated by very intense irradiance; the harmonic generation is one of the most interesting topics for both fundamental understanding and plasma applications. Forthcoming papers will deal with both of these aspects.

[1] P. Maine, D. Strickland, P. Bado, M. Pessot, and G.MOurou, IEEE J. Quantum Electron. **24**, 398 (1988); M. Ferray, L. A. Lompré, O. Gobert, G. Mainfray, C. Manus, A. Sanchez, and A. Gomes, Opt. Commun. **75**, 278 (1990); M. D. Perry, F. G. Patterson, and J. Weston, Opt. Lett. **15**, 381 (1990); J. P. Watteau, G. Bonnaud, J. Coutant, R. Dautray, A. Decoster, M. Louis-Jacquet, J. Ouvry, J. Sauteret, S. Seznec, and D. Teychenné, Phys. Fluids B **4**, 2217 (1992).

[2] T. Tajima and J. M. Dawson, Phys. Rev. Lett. **43**, 267 (1979); C. Joshi, W. B. Mori, T. Katsouleas, J. M. Dawson, J. M. Kindel, and D. W. Forslund, Nature **311**, 525 (1984); L. M. Gorbunov and V. I. Kirsanov, Zh. Eksp. Teor. Fiz. **93**, 509 (1987) [Sov. Phys. JETP **66**, 290 (1987)]; P. Sprangle, E. Esarey, A. Ting, and G. Joyce, Appl. Phys. Lett. **53**, 2146 (1988); D. Teychenné, G. Bonnaud, and J. L. Bobin, Phys. Rev. E **48**, 3248 (1993).

[3] B. I. Cohen, A. N. Kaufman, and K. M. Watson, Phys. Rev. Lett. **29**, 581 (1972); M. N. Rosenbluth and C. S. Liu, *ibid.* **29**, 701 (1972); C. M. Tang, P. Sprangle, and R. N. Sudan, Appl. Phys. Lett. **45**, 375 (1984); J. L. Bobin, Ann. Phys. (France) **11**, 593 (1986) (in French); IEEE Trans. Plasma Sci. **PS-15**, 85 (1987); contributions from T. Katsouleas, W. B. Mori, C. Darrow, C. Joshi, D. Umstadter, C. E. Clayton, S. H. Batha, C. J. McKinstrie, S. J. Karttunen, and R. R. E. Salomaa; *New Developments in Particle Acceleration Techniques, Conference Proceedings, Orsay, 1987,* edited by S. Turner (CERN, Genève, 1987), Vol. II.

[4] C. E. Clayton *et al.*, Phys. Rev. Lett. **54**, 2343 (1985); A. E. Dangor, A. K. L. Dymoke-Bradshaw, A. Dyson, T. Garvey, I. Mitchell, A. J. Cole, C. N. Danson, C. B. Edwards and R. G. Evans, IEEE Trans. Plasma Sci. **PS-15**, 161 (1987); A. Ebrahim, Phys. Canada **45**, 178 (1989); Y. Kitagawa *et al.*, Phys. Rev. Lett. **68**, 48 (1992); F. Amiranoff *et al.*, *ibid.* **68**, 3710 (1992).

[5] C. E. Clayton, K. A. Marsh, A. Dyson, M. Everett, A. Lal, W. P. Leemans, R. Williams, and C. Joshi, Phys. Rev. Lett. **70**, 37 (1993).

[6] A. L. Harvey, Phys. Rev. D **6**, 1474 (1972).

[7] L. A. Mc Coll, Am. J. Phys. **25**, 525 (1957).

[8] I. S. Gradhshteyn and I. M. Ryzhik, *Table of Intergrals, Series and Products* (Academic, London, 1980).

[9] S. Wolfram, *Mathematica* (Addison-Wesley, Redwood City, CA, 1991), Version 2.

[10] L. Landau and E. Lifchitz, *Physics Theory, Mechanics* (Mir, Moscow, 1982), Vol. 1.

[11] J. M. Rax and N. J. Fisch, Phys. Fluids B **4**, 1323 (1992).

[12] P. Mora and F. Amiranoff, J. Appl. Phys. **66**, 3476 (1989).